

# Amaranth Food Dye Photochemical and Photoelectrochemical Degradation: Experiments and Mathematical Modelling

CRISTIANO P. SILVA, SANDRO MARMITT, CLAUS HAETINGER AND SIMONE STÜLP

Programa de Pós-Graduação em Ambiente e Desenvolvimento (PPGAD),  
Univates,  
Avelino Tallini, 171, Lajeado/RS,  
BRAZIL.  
<http://www.univates.br/ppgad>  
[stulp@univates.br](mailto:stulp@univates.br)

*Abstract:* - This paper studied the photochemical and photoelectrochemical degradation of food dye (red dye - amaranth). The investigation aimed at the assessment of alternative treatments, focusing the use of clean technologies. The photochemical and photoelectrochemical degradation experiments were performed in a compartment with UV radiation (mercury lamp – 125W). For the photoelectrochemical degradation, the best mathematical modelling indicated by the LAB Fit software was the exponential model. This behavior indicates a first-order reaction. On the other side, the best mathematical model for the photochemical degradation was the linear one. Therefore, the photochemical degradation indicates a zero-order reaction. For the amaranth dye, the photoelectrochemical method showed itself to be more efficient than the photochemical one. The photoelectrochemical treatment pointed to a 92% color reduction in the dye solution, and Chemical Oxygen Demand (COD) removal reached up to 57%.

*Key-Words:* - food dye, photoelectrochemical degradation, azo group, kinetics, UV radiation.

## 1 Introduction

Advanced oxidation processes (AOPs) which involve in situ generation of highly potent chemical oxidants, such as the hydroxyl radical ( $\bullet\text{OH}$ ), have emerged as an important class of technologies for accelerating the oxidation (and hence contaminant removal) of a wide range of organic contaminants in polluted water and air [1].

These techniques were used in effluents with organic material in high concentration.

The advanced oxidation methods use oxidation agents, like, ozone, with its high redox potential  $E_0 = 2.07 \text{ V}$  and its electrophilic properties, for disinfection and oxidation of organic and inorganic compounds [2].

In general, the methods of advanced oxidation [3] include application of the following agents: ozone [4, 5], hydrogen peroxide, UV radiation [6], ozone and UV radiation together [7], hydrogen peroxide and UV radiation [8], Fenton [9] reagent and hydrogen peroxide, and photocatalysis on titanium dioxide. All the methods listed above were used in the investigation of the oxidation, and some of them were applied in the treatment of various kinds

of wastewater [10].

Although the removal and eventual mineralization of organic contaminants through advanced oxidation processes can be complex, and involves a number of elementary chemical steps, the overall kinetics or removal rate of a specific component, can often be described phenomenologically by simple rate expressions that are either zero-order or first-order in the organic contaminant [1].

Over the last decades, the increasing industry demand for dyes has shown a high pollutant potential, specially the use of azo dyes (Fig. 1) [11], for example, tartrazine [12], amaranth [13] and other. Decoloration is one of the basic indicators that describe the quality of water [14].

The food industry grows up very fast over around the world, increasing its sales each year more and more [15]. Although this is economically good, the high competitiveness of the sector makes the factories to improve their products making them more attractive. Meanwhile they usually use synthetic dyes to achieve their goals [16, 17, 18] because the color of the food influences the consumer's likes [19, 20]. These

synthetic food dyes are most widely composed by aromatic rings and chromophore groups (e.g. azo, anthraquinone) [21, 22], and present high stability and xenobiotic characteristics, hence they are not easily degraded by conventional biological treatment processes [11], [23, 24]. For the environmental, the minimization of waste represents the ultimate solution to pollution problems that threaten ecosystems at global and regional levels [24].

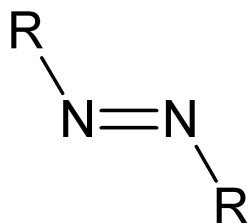


Fig. 1 Azo group chemical structure.

Photolysis (UV irradiation) is an alternative method for the degradation of azo dyes [25, 26].

Photodegradation of amaranth has been reported in the literature [12, 13, 14]. The degradation has been investigated using UV radiation in the presence of  $\text{TiO}_2$ . The results showed an efficient degradation through photocatalytic treatment.

This work aimed to verify the possibility of use of the photochemical and photoelectrochemical techniques to degrade amaranth dye (FD&C Red No. 2) [27, 28] and compared the degradation kinetics [29, 30] (mathematical modelling) and efficiency. In some countries this food dye is not permitted, for example in Russian [25]. On the other hand, the dye is still allowed in other countries, including Brazil [31]. The photoelectrochemical degradation of dye solutions was investigated using DSA (Dimensionally Stable Anodes) [32, 33]. This is a type of anode where oxidation reactions usually will be acting on dye via  $\text{HO}\cdot$  radicals on the surface, which can lead to better performance in organic and inorganic species degradation [34].

## 2 Experimental

### 2.1 Reagents

Red amaranth (95%) dye (C.I. 16185) [35] was acquired from Duas Rodas (Santa Catarina, Brazil) as a commercially available dye formulation and used without further purification. This dye is an azo type dye as represented by the chemical structure in Fig. 2. The studies were carried out on  $100 \text{ mg L}^{-1}$  aqueous dye solutions in the presence of

$0.1 \text{ mol L}^{-1} \text{ KNO}_3$  support electrolyte.

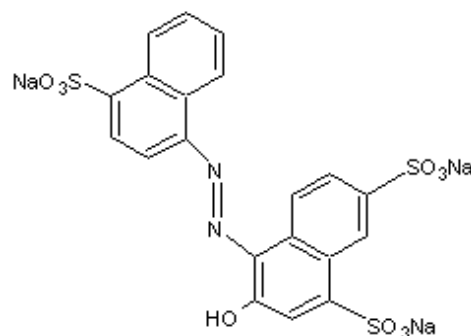


Fig. 2. Amaranth dye chemical structure.

### 2.2 Photoelectrochemical and photochemical treatments

Experiments were performed in an open batch system [35]. The system consisted a 200 mL quartz cell and the solution was irradiated with an ultraviolet lamp (125 W) [36] during 90 minutes. In photoelectrochemical treatment DSA  $\text{Ti/Ru}_{0.3}\text{Ti}_{0.7}\text{O}_2$  electrodes ( $11.2 \text{ cm}^2$ ) and a potentiostat CIDPE EQ030C (Fig. 3) were used. The photoelectrochemical experiments were performed at a  $20 \text{ mA cm}^{-2}$  current density.

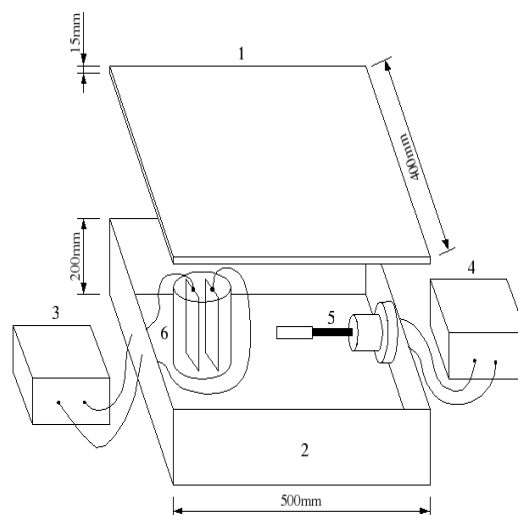


Fig. 3 Schematic photochemical and photoelectrochemical system: 1,2 – box, 3 – potentiostat, 4 – lamp reactor, 5 - ultraviolet lamp (125 W) and 6 - quartz cell with or without DSA electrodes.

### 2.3 Mathematical modelling

The mathematical treatment of the experimental data was made using the LAB Fit Curve Fitting software [37]. The tolerance of the non-linear regressions, accomplished by the least square method, was fixed by  $1 \cdot 10^{-6}$ , and the quality of the fittings was indicated by the determination and the reduced  $\chi^2$  coefficients [38]. The performance of the software has been verified with the Statistical Reference Datasets Project (SRDP) of the National Institute of Standards and Technology (NIST) [39].

Regression analyses [40] of plotted data were carried out using Microcal Origin 5.0 (Microcal Software) [41].

### 2.4 Analytical methodology

The analytical analyses in aqueous dye solutions were realized before and after the photochemical and photoelectrochemical treatments.

The UV/Vis spectrophotometer used for the determination of dye disappearance kinetics was a "Perkin Elmer Lambda 25" UV/Vis Spectrometer recording the spectra over the 190-900 nm.

Chemical Oxygen Demand (COD) was made using a method described in Standard Methods [42]. In the COD test, the organic material concentration is calculated from the oxidant consumption necessary for the oxidation of the organic material, using a very strong inorganic oxidant.

The Chromatographic experiments were performed using an Agilent Technologies 1200 Series Quaternary LC System and Diode-Array Detector (DAD). The mobile phase used was a mixture of water and methanol in the volumetric proportion of 70:30 [17]. The flow rate used was  $0.5 \text{ mL min}^{-1}$  and detect43, 44]. The analytical column [12] was Zorbax Eclipse XDB-C18 4.6 mm diameter and 150 mm length,  $5 \mu\text{m}$ .

## 3 Results and Discussion

The efficiency of photoelectrochemical and photochemical degradation of amaranth dye was first investigated using UV-Vis spectra and monitored the disappearance of this compound. Amaranth dye absorbed in the visible region ( $\lambda = 525\text{nm}$ ) [17]. Fig. 4 and 5 show the absorbance spectra (scan) during photoelectrochemical and photochemical treatments, respectively.

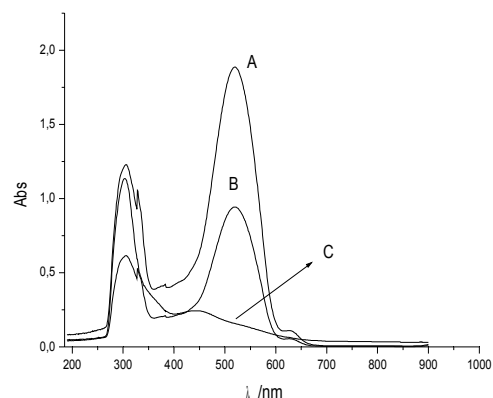


Fig. 4. UV-Vis absorption spectra of  $100\text{mg L}^{-1}$  amaranth before (A) and after photoelectrochemical treatment time 45 min (B) and time 90 min (C).

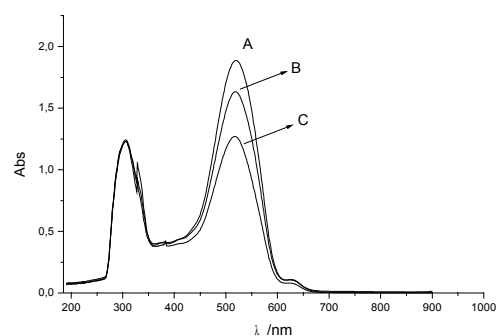


Fig. 5. UV-Vis absorption spectra of  $100\text{mg L}^{-1}$  amaranth before (A) and after photochemical treatment time 45 min (B) and time 90 min (C).

In these treatments (photochemical and photoelectrochemical) times, the disappearance of long wavelength absorbing chromophores in the dye structure was around 34% and 92%, respectively. Fig. 6 shows the absorbance ( $\text{Abs}_t/\text{Abs}_0$ ) during the degradation period, for both photochemical and photoelectrochemical degradation.

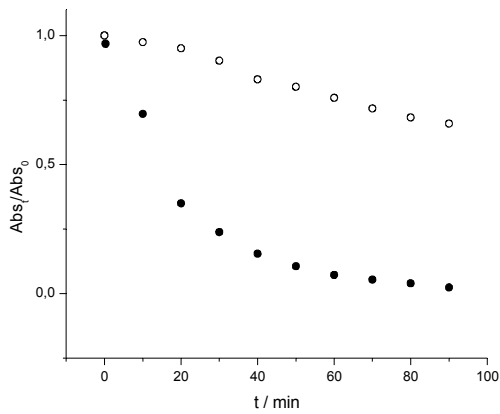


Fig. 6. Amaranth absorbance reduction as a function of photochemical (○) and photoelectrochemical (●) treatment time ( $\lambda = 525\text{nm}$ ).

For the photoelectrochemical degradation, the best mathematical modelling indicated by the LAB Fit software was the exponential model  $y(t) = 1.01538 \cdot 0.954557^t$ , where  $y$  indicated  $\text{Abs}_t/\text{Abs}_0$ , with coefficients  $R^2 = 0.99263$  and reduced  $\chi^2 = 0.000885426$ . This behavior indicates a first order reaction.

The first-order rate law [45] for the disappearance of some reactant A is given by

$$-\frac{d[A]}{dt} = k \cdot [A], \quad (1)$$

where  $k$  is a constant.

This differential equation rearranges to

$$\frac{1}{[A]} d[A] = -k dt, \quad (2)$$

which can be integrated directly. Once (at  $t = 0$ ) the concentration of A is initially  $[A]_0$  and at a later time  $t$  it is  $[A]_t$ , we write

$$\ln\left(\frac{[A]_t}{[A]_0}\right) = -k \cdot t, \quad (3)$$

or equivalently,

$$[A]_t = [A]_0 \cdot e^{-kt}. \quad (4)$$

The latter shows that in a first-order reaction the reactant concentration decreases exponentially with time, with a rate determined by  $k$ . The former shows that if it is plotted against  $t$ , then a first-order reaction will give a straight line [46]. If the plot is straight, then the reaction is first-order, and the value of  $k$  may be obtained from the slope (the slope is  $-k$ ).

Let now  $a=1.01538$ ,  $b=0.954557$  and  $[A]_0 = 1$ .

We have found  $[A]_t = [A]_0 \cdot e^{-kt} = a \cdot b^t$ , for

every  $t$ . In particular, for  $t=1$ , an easy calculation

gives  $k = -\ln\left(\frac{a \cdot b}{[A]_0}\right) = -0.031245$ . The Figure

7 shows  $y(t) = \ln\left(\frac{\text{Abs}_t}{\text{Abs}_0}\right)$  for the

photoelectrochemical treatment.

When  $\ln\left(\frac{[A]_t}{[A]_0}\right)$  is plotted against  $t$ , then a first-order reaction will give a straight line [45, 46] ( $[A]_t = [A]_0 \cdot e^{-kt} = a \cdot b^t$ ), and the value of  $k$  may be obtained from the slope (the slope is  $-k$ ).

Let now  $a=1.01538$ ,  $b=0.954557$  and  $[A]_0 = 1$ . In particular, for  $t=1$ , an easy calculation gives

$k = -\ln\left(\frac{a \cdot b}{[A]_0}\right) = -0.031245$ . The Fig. 7 shows

$k = -\ln\left(\frac{a \cdot b}{[A]_0}\right) = -0.031245$  for the

photoelectrochemical treatment.

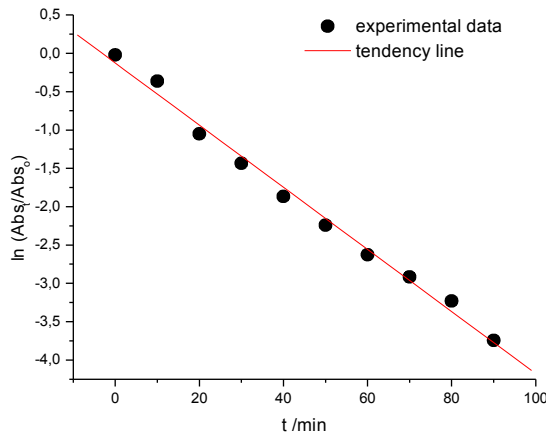


Fig. 7. Kinetics of amaranth dye disappearance during photoelectrochemical degradation process.

The photoelectrochemical degradation exhibits first-order decay, with a linear dependence of  $\ln\left(\frac{Abs_t}{Abs_0}\right)$  on time, given by  $y(t) = -0.04065 \cdot t - 0.1182$ ; therefore, the observed first-order rate. This result is in according to literature [47]. The constant  $k$  was  $0.04065 \text{ min}^{-1}$  for this treatment. However, others authors [27] explain the amaranth dye degradation and in this case the  $k$  was around  $0.006 \text{ min}^{-1}$ , approximately one order greater.

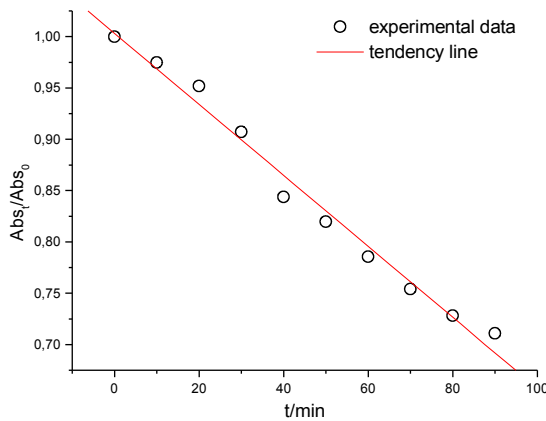


Fig. 8. Kinetics of amaranth dye disappearance during photochemical degradation process.

On the other side, the best mathematical model for the photochemical degradation of Fig. 6 was the linear one, given by  $y(t) = -0.0040834 \cdot t + 1.01145$ , with  $R = -0.9946991$  and reduced  $\chi^2 = 0.000183776$ . Therefore, the photochemical degradation indicates a zero-order reaction [48, 49], where  $\frac{d[A]}{dt} = k$ . This can also occur in a photochemical reaction if the rate is determined by the light intensity; in this case

$k$  may be proportional to the light intensity [46].

The figure-of-merit [1] *Electric Energy per Order* ( $E_{EO}$ ) is best used for situations where the mechanism involves first-order reaction. For the photoelectrochemical treatment the  $E_{EO}$  was  $854.99 \text{ kWh.m}^{-3}$ . The *Electric Energy per Mass* ( $E_{EM}$ ) is most useful when were zero-order reactions take place. This figure-of-merit is most useful when concentration is high because the removal rate of the contaminant is directly proportional to the electric energy rate. For the photochemical treatment the  $E_{EM}$  was  $14204.54 \text{ kWh.kg}^{-1}$ . These results demonstrate the photoelectrochemical efficiency.

The  $E_{EO}$  values can be calculated using the following formula:

$$E_{EO} = \frac{P \cdot t \cdot 1000}{V \cdot \log\left(\frac{c_i}{c_f}\right)} \quad (5)$$

where:

$P$  = is the rated power [kW];

$t$  = time [h];

$V$  = is the volume [L] of effluent treated;

$c_i$  = the initial (or influent) concentrations [M or mol  $L^{-1}$ ] of C;

$c_f$  = the final (or effluent) concentrations [M or mol  $L^{-1}$ ] of C.

For the photoelectrochemical treatment the  $E_{EO}$  was  $854.99 \text{ kWh.m}^{-3}$ . The  $E_{EM}$  value [kWh/kg] can be calculated from the simple formula:

$$E_{EM} = \frac{P \cdot t \cdot 1000}{V \cdot M \cdot (c_i - c_f)} \quad (6)$$

where:

$P$  = is the rated power [kW];

$t$  = time [h];

$V$  = is the volume [L] of effluent treated;

$M$  = is the molar mass [ $\text{g mol}^{-1}$ ]

$c_i$  = the initial (or influent) concentrations [ $M$  or  $\text{mol L}^{-1}$ ] of  $C$ ; Alternatively, if mass concentrations are used ( $\gamma = m/V$ ) (usual unit  $\text{mg/L}$ );

$c_f$  = the final (or effluent) concentrations [ $M$  or  $\text{mol L}^{-1}$ ] of  $C$ ; Alternatively, if mass concentrations are used ( $\gamma = m/V$ ) (usual unit  $\text{mg/L}$ ).

In Chemical Oxygen Demand (COD) measurements (Fig. 9), a 47% and 57% percentage reduction occurred for the photochemical and photoelectrochemical treatments, respectively. These results indicate an organic material degradation beyond the color decrease of amaranth dye solution [50].

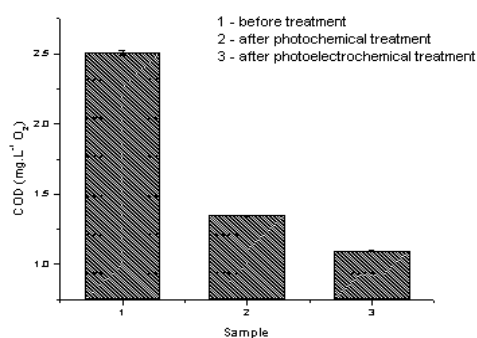


Fig. 9 Influence of treatment (photochemical or

photoelectrochemical) in COD elimination.

The Fig. 10 shows the chromatographic amaranth dye behavior before and after photoelectrochemical treatment at 260 nm, and the Fig. 11 before and after degradation treatment at 525 nm.

In regions near 260 nm, a peak decreases after the photoelectrochemical treatment (Fig. 10). This may indicate the presence of aromatic amines [51, 52, 53] in accordance with the COD results (57%), showing a non-complete degradation (mineralization) of organic material [53].

The Fig. 11 shows a peak decrease in 2.87 minutes (retention time) at 525 nm [54, 20]. The concentrations were  $100 \text{ mg L}^{-1}$  (before treatment), and  $19.81 \text{ mg L}^{-1}$  after photoelectrochemical treatment.

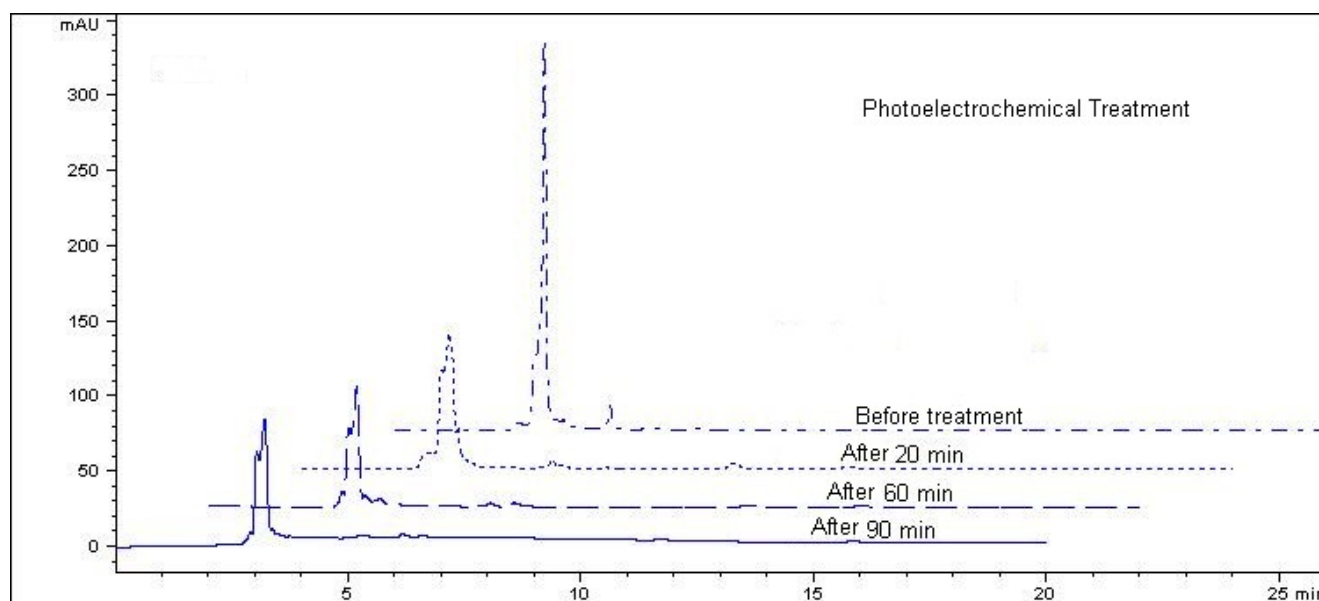


Fig. 10 Chromatogram of the separation in a C18 column of amaranth, before and after the photoelectrochemical degradation. The chromatographic conditions are given in the text.  $\lambda = 260 \text{ nm}$ .

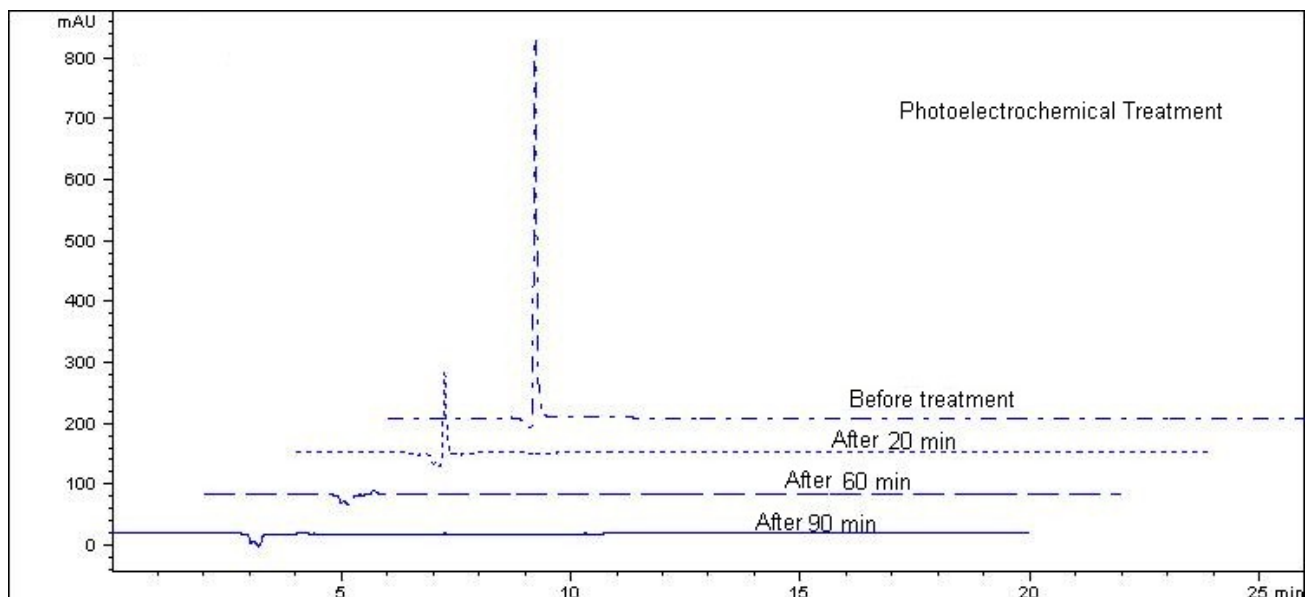


Fig 11 Chromatogram of the separation in a C18 column of amaranth, before and after the photoelectrochemical degradation. The chromatographic conditions are given in the text.  $\lambda = 525$  nm.

The Fig. 12 shows the chromatographic amaranth dye behavior before and after photochemical treatment at 260 nm, and the Fig. 13 before and after degradation treatment at 525 nm.

In regions near 260 nm, a peak decreases after the photochemical treatment (Fig. 12). This may indicate the presence of aromatic amines [51, 52, 53] in accordance with the COD results (47%), showing a not complete degradation

(mineralization) of organic material.

The Fig. 13 shows a peak decrease in 2.87 minutes (retention time) at 525 nm [54, 20]. The concentrations were  $100 \text{ mg L}^{-1}$  (before treatment) and  $49.23 \text{ mg L}^{-1}$ , after photochemical treatment. The photoelectrochemical treatment was less efficient, in accordance with the absorbance and COD results.

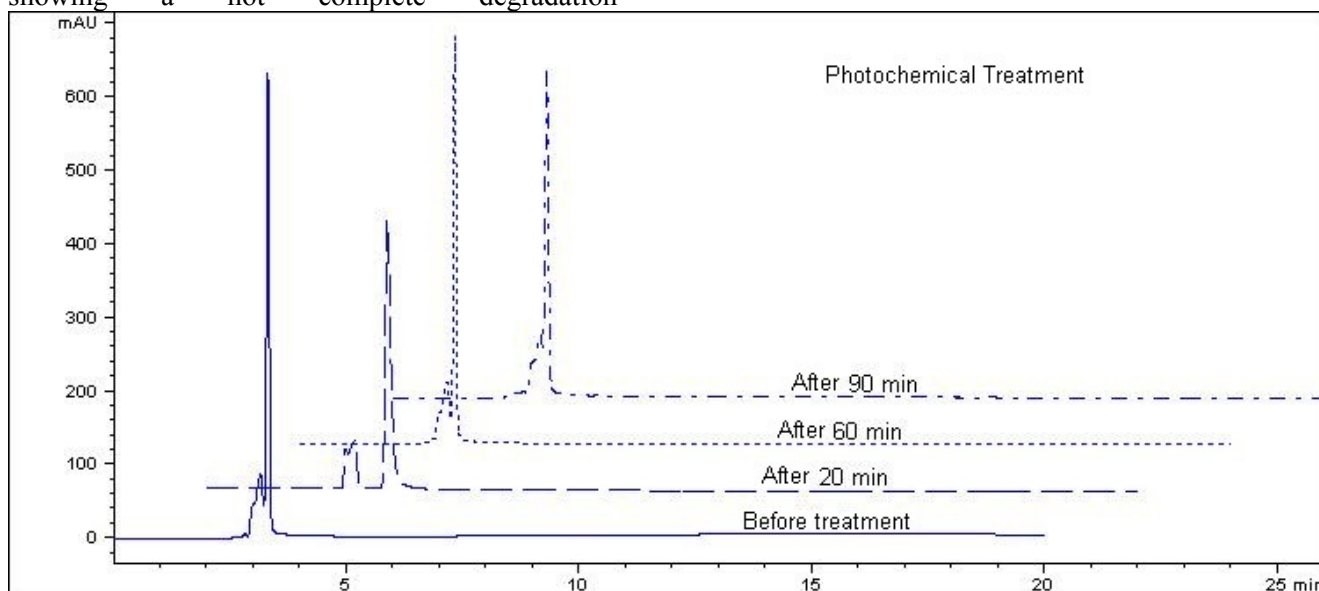


Fig 12 Chromatogram of the separation in a C18 column of amaranth, before and after the photochemical degradation. The chromatographic conditions are given in the text.  $\lambda = 260$  nm.

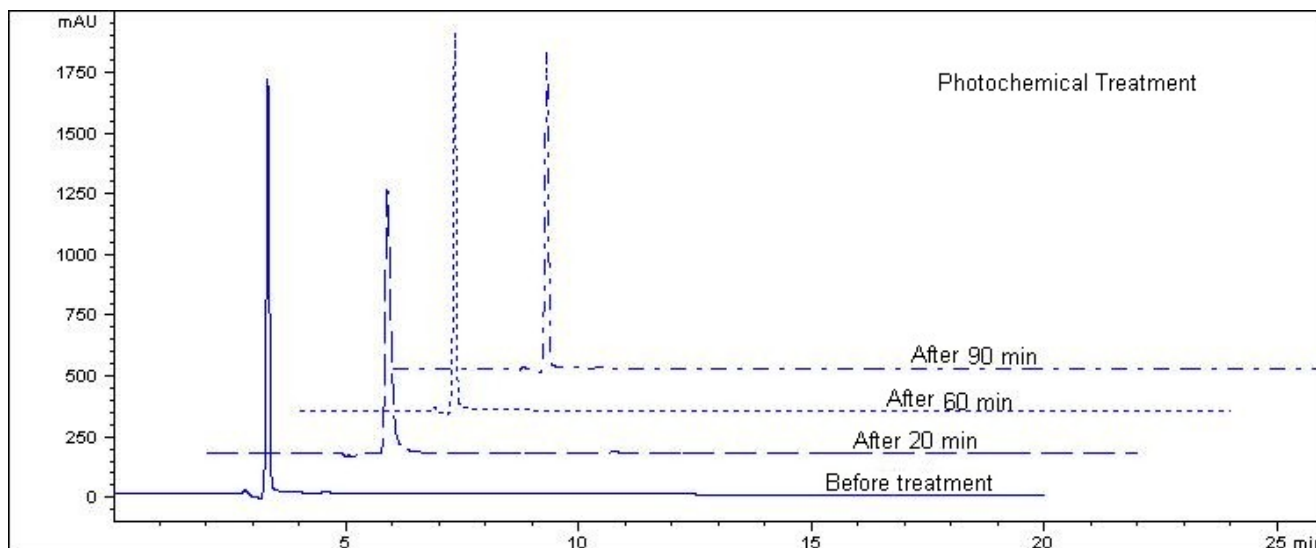


Fig 13 Chromatogram of the separation in a C18 column of amaranth, before and after the photochemical degradation. The chromatographic conditions are given in the text.  $\lambda = 525$  nm.

The Fig. 14 and Fig.15 show a comparison between the amaranth dye before and after photochemical and photoelectrochemical treatments, in 260 and 525 nm. These results suggest that the amaranth solution after the photochemical degradation is more toxic (increase

of aromatic amines in relationship to photoelectrochemical treatment), indicating that the process may be envisaged as a method for treatment of colored wastewaters for decolorization and degradation, in particular food industries.

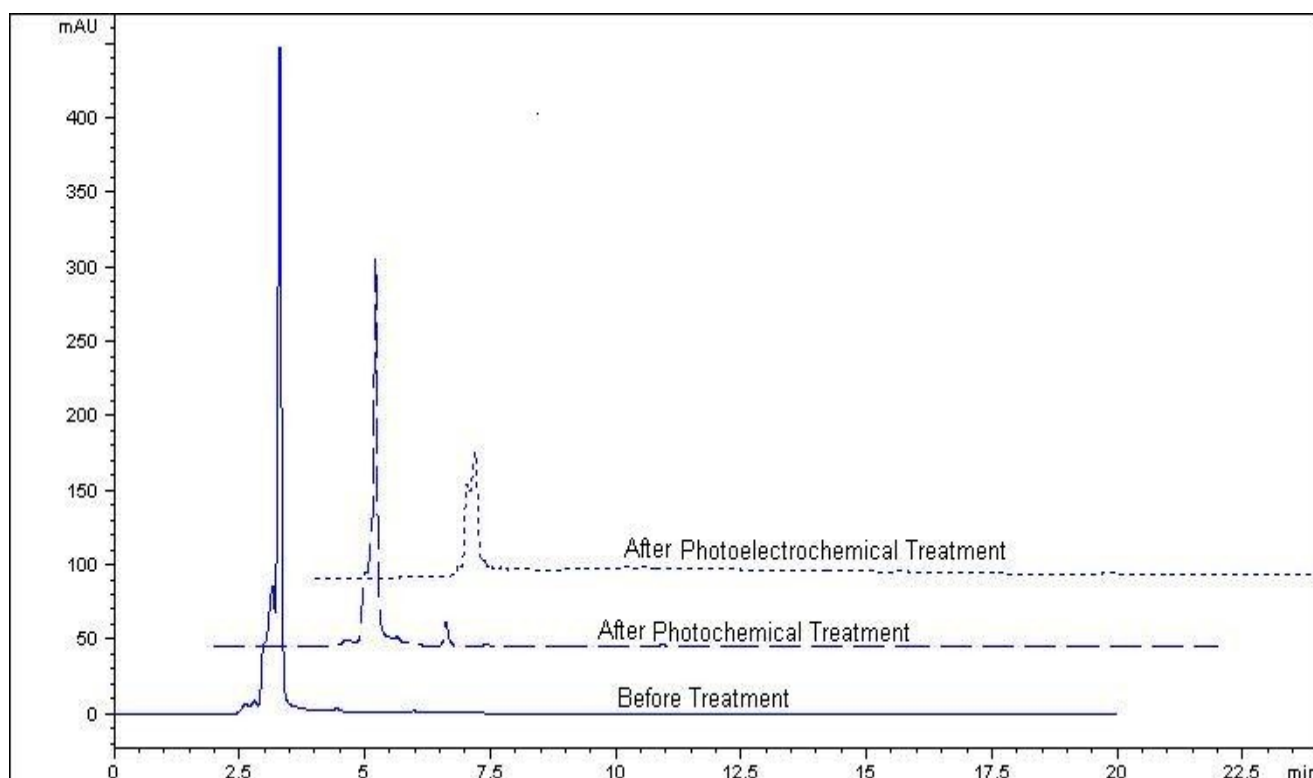


Fig. 14. Chromatogram of the separation in a C18 column of amaranth. The chromatographic conditions are given in the text.  $\lambda = 260$  nm.

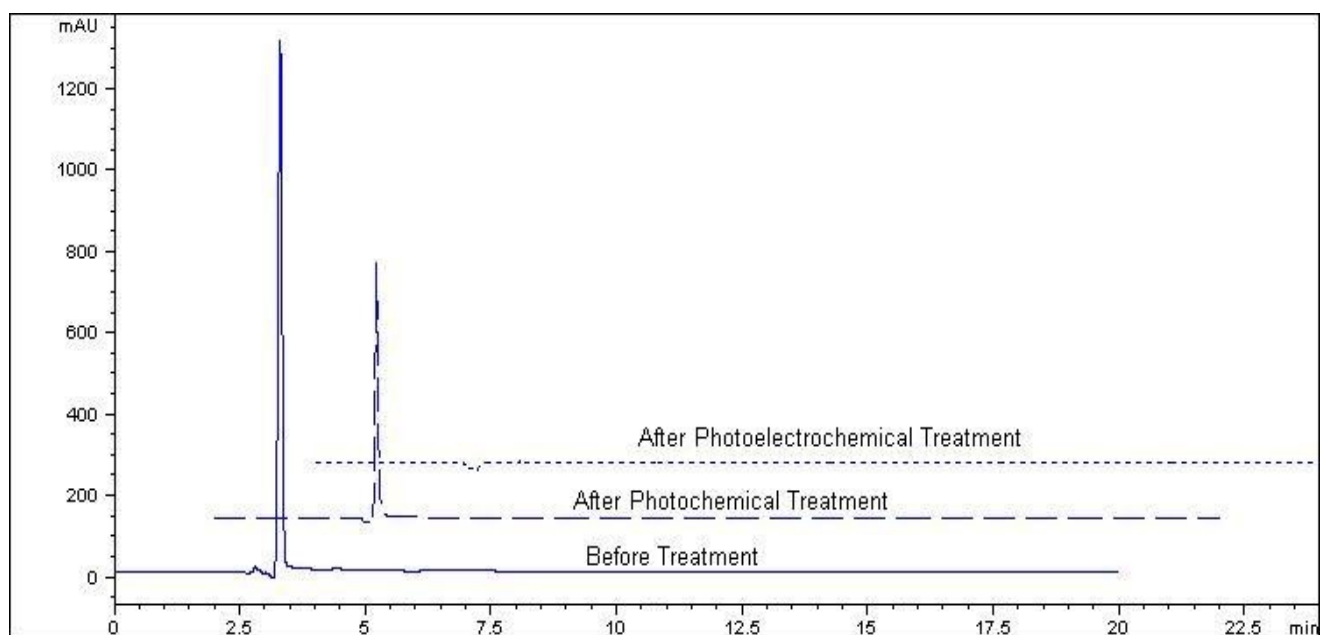


Fig. 15. Chromatogram of the separation in a C18 column of amaranth. The chromatographic conditions are given in the text.  $\lambda = 525$  nm.

These results suggest that the chromophore degradation step followed the same mechanism in both treatments (photochemical and photoelectrochemical), probably involving  $-N=N-$  group reduction. The photoelectrochemical treatment was more efficient, in accordance with the absorbance and COD results.

## 4 Conclusion

The results presented here show that for the amaranth dye, the photoelectrochemical method was considered more efficient than the photochemical one. The photochemical treatment showed a 92% color reduction in the dye solution, and Chemical Oxygen Demand (COD) removal reached 57%. For the photoelectrochemical degradation, the best mathematical modelling indicated by the LAB Fit software was the exponential model. This behavior indicates a first-order reaction. On the other side, the best mathematical model for the photochemical degradation was the linear one. Therefore, the photochemical degradation indicates a zero-order reaction.

These results suggest that photoelectrochemical process may be envisaged as a method for treatment of colored wastewaters for decolorization and degradation, in particular food industries.

## 5 Acknowledgments

The authors would like to acknowledge financial support from FAPERGS and UNIVATES.

## References:

- [1] J. R. Bolton, K.G. Bircher, W. Tumas, C.A. Tolman, Figures-of-merit for the technical development and application of advanced oxidation technologies for both electric- and solar-driven systems, *Pure and Applied Chemistry*, Vol. 73, No. 4, 2001, pp. 627-637.
- [2] K. Patrik, G. Ernst, H. E. Siegfried,  $TiO_2$  photocatalytic oxidation of monochloroacetic acid and pyridine: influence of ozone, *Journal of Photochemistry and Photobiology A: Chemistry* Volume 136, Issue 3, 29 September 2000, Pages 163-168
- [3] J. Perkowski, S. Ledakowicz, Decomposition of Antraquinone dye in the aqueous solution during advanced oxidation processes, *Fibres & Textiles in Eastern Europe*, Vol. 10, 2002, pp. 68-72.
- [4] G. Gualtieri, F. Calastrini, C. Busillo, G. Pirovano, The RAMS-CALMET-CALGRID modelling system to assess seasonal ozone pollution: a five-month application over Tuscany region, *WSEAS Transactions on Environment and Development*, Issue 11, Volume 3, November 2007, 196-205.
- [5] A. Psaroudaki, An extensive survey of the impact of tropospheric ozone on the biochemical properties of edible plants, *WSEAS Transactions on Environment and Development*, Issue 6, Volume 3, June 2007, 99-110.
- [6] R. Bertazzoli, R. Pelegrini, Photoelectrochemical discoloration and degradation of organic pollutants in aqueous solutions, *Química Nova*, Vol. 25, No3., 2002, pp. 477-482.

- [7]M. Dilmeghani, K.O. Zahir, Kinetics and mechanism of chlorobenzene degradation in aqueous samples using advanced oxidation processes, *Journal of Environmental Quality*, Vol. 30, 2001, pp. 2062-2070.
- [8]F. V. F. Araújo, L. Yokoyama, Color removal in reactive dye solutions by UV/H<sub>2</sub>O<sub>2</sub> Oxidation, *Química Nova*, Vol. 29, No. 1, 2006, pp. 11-14.
- [9]A. CK. Yip, F. LY. Lam, X. Hu, A novel heterogeneous acid-activated clay supported copper catalyst for the photobleaching and degradation of textile organic pollutant using photo-Fenton-like reaction, *Chemical Communications*, Vol. 25, 2005, pp. 3218-3220.
- [10]L.S. Andrade, E.A. Laurindo, R.V. Oliveira, R.C. Rocha-Filho, Q.B. Cass, Development of a HPLC method to follow the degradation of phenol by electrochemical or photoelectrochemical treatment, *Journal of the Brazilian Chemical Society*, Vol. 17, No. 2, 2006, pp. 369-373.
- [11]W.S. Pereira, R.S. Freire, Azo dye degradation by recycled waste zero-valent iron powder, *Journal of the Brazilian Chemical Society*, Vol. 17, No. 5, 2006, pp. 832-838.
- [12]E.C. Vidotti, M.C.E. Rollemberg, Derivative spectrophotometry: A simple strategy for simultaneous determination of food dyes, *Química Nova*, Vol. 29, No. 2, 2006, pp. 230-233.
- [13]A. Keck, J. Klein, M. Kudlich, A. Stolz, H-J. Knackmuss, R. Mattes, Reduction of azo dyes by redox mediators originating in the naphthalenesulfonic acid degradation pathway of *Sphingomonas sp.* Strain BN6, *Applied and Environmental Microbiology*, Vol. 63, No. 9, 1997, pp. 3684-3690.
- [14]J. Perkowski, L. Kos, Decolouration of model dyehouse wastewater with advanced oxidation processes, *Fibres & Textiles in Eastern Europe*, Vol. 11, No.3, 2003, pp. 67-71.
- [15]<http://www.abia.org.br/noticias.asp>, accessed in May 2008.
- [16]Prado, M.; Abujamra, F.; Godoy, H. Análise de corantes em chás aromatizados. *Revista Analytica*, No. 5, 2003, pp. 31-35.
- [17]M.A. Prado, H.T. Godoy, Contents of synthetic in foods determined by high performance liquid chromatography, *Química Nova*, Vol. 30, No. 2, 2007, pp. 268-273.
- [18]F. A. R. Barros, P. C. Stringheta, Microencapsulamento de Antocianinas – Uma alternativa para o aumento da aplicabilidade como ingrediente alimentício. *Biotecnologia Ciência e Desenvolvimento*, No. 36, 2006, pp. 18-24.
- [19]P. B. L. Constant, P. C. Stringheta, D. Sandi, Corantes Alimentícios. *Boletim do Centro de Processamento de Alimentos*, Vol. 20, No. 2, 2002, pp. 203-220.
- [20]M.A. Prado, H.T. Godoy, Determination of synthetic dyes by high performance liquid chromatography (HPLC) in jelly powder, *Química Nova*, Vol. 27, No. 1, 2004, pp. 22-26.
- [21]Guaratini, C. C. I.; Zanoni, M. V. B. Textile dyes. *Química Nova*, Vol. 30, No. 1, 2000, pp. 71-78.
- [22]A. Kunz, P. Peralta-Zamora, S. G. Moraes, N. Durán, New tendencies on textile effluent treatment. *Química Nova*, Vol. 25, No. 1, 2002, pp. 78-82.
- [23]D. F. Angelis, C. R. Corso, E. D. Bidoia, P. B. Moraes, R. N. Domingos, R. C. Rocha-Filho, Electrolysis of polluting wastes. I - Wastewater from a seasoning freeze drying industry. *Química Nova*, Vol. 21, No. 1, 1998, pp. 20-24.
- [24]U. N. Ngoc, H. Schnitzer, Zero emissions systems in food processing industry, *WSEAS Transactions on Environment and Development*, Issue 4, Vol. 4, 2008, pp. 313-333.
- [25]M. Karkmaz, E. Puzenat, C. Guillard, J.M. Herrmann, Photocatalytic degradation of the alimentary azo dye amarant mineralization of the azo group to nitrogen, *Applied Catalysis B: Environmental*, Vol. 51, 2004, pp. 183-194.
- [26]C-H. Wu, Comparison of azo dye degradation efficiency using UV/single semiconductor and UV/coupled semiconductor systems, *Chemosphere*, Vol. 57, 2004, pp. 601-608.
- [27]M. Abu Tariq, M. Faisal, M. Munner, Semiconductor-mediated photocatalysed degradation of two selected azo dye derivatives, amarant and bismark brown in aqueous suspension, *Journal of Hazardous Materials*, Vol. 58, No. 1, 2005, pp. 172-179.
- [28]<http://www.fda.gov/default.htm>, accessed in September 2007.
- [29]Th. Fink, J.-P. Dath, R. Imbihl, and G. Ertl, Kinetic oscillations in the NO + CO reaction on Pt(100): Experiments and mathematical modeling, *Journal of Chemical Physics*, 95 (3), 1 August 1991, 2109-2126.
- [30]S. Simkins, M. Alexander, Models for Mineralization Kinetics with the Variables of Substrate Concentration and Population Density, *Applied and Environmental Microbiology*, June 1984, p. 1299-1306, Vol. 47, No. 6.
- [31]<http://www.anvisa.gov.br>, accessed in September 2007.
- [32]B. Wang, W. Kong, H. Ma, Electrochemical treatment of paper mill wastewater using three-dimensional electrodes with Ti/Co/SnO<sub>2</sub>-Sb<sub>2</sub>O<sub>5</sub> anode, *Journal of Hazardous Materials*, Vol. 146, 2007, pp. 295-301.
- [33]G.R.P. Malpass, A.J. Motheo, Cyclic

- Voltammetric behaviour of Dimensionally Stable Anodes in the presence of C1-C3 Aldehydes, *Journal of the Brazilian Chemical Society*, Vol. 14, No. 4, 2003, pp. 645-650.
- [34]P.A. Carneiro, Fugivara, C.S., R.F.P. Nogueira, N. Boralle, M.V.B. Zanoni, A comparative study on chemical and electrochemical degradation of reactive blue 4 dye, *Portugaliae Electrochimica Acta*, Vol. 21, 2003, pp. 49-67.
- [35]C.P. Silva, S. Marmitt, C. Haetinger, S. Stülp, Assessment of red dye degradation through photochemical process, *Engenharia Sanitária e Ambiental*, Vol. 13, No. 1, 2008, pp. 73-77.
- [36]S. Stülp, C. P. Silva, S. Marmitt, The use of electrochemical techniques in the treatment of food industry effluents: a tool for the environmental management systems, *Estudo & Debate*, Vol. 12, No. 2, 2005, pp. 109-123.
- [37]<http://www.labfit.net>, accessed in September 2007.
- [38]P.R. Bevington, D.K. Robinson, Data reduction and error analysis for the physical sciences. Boston: WCB/McGraw-Hill, second edition, 328p, 1992.
- [39]W.P. da Silva, C.M.D.P.S. e Silva, C.G.B. Cavalcanti, D.D.P.S. e Silva, I.B. Soares, J.A.S. Oliveria, C.D.P.S. e Silva, LAB Fit ajuste de curva: um software em português para tratamento de dados experimentais (LAB Fit curve fitting: a software in portuguese for treatment of experimental data), *Revista Brasileira de Ensino de Física* 26(4) (2004), pp. 419-427, [www.sbfisica.org.br](http://www.sbfisica.org.br)
- [40]W. J. Arion, W. K. Canfield, E. S. Callaway, H.-J. Burger, H. Hemmerle, G. Schubert, A. W. Herling, R. Oekonomopulos, Direct Evidence for the Involvement of Two Glucose 6-Phosphate-binding Sites in the Glucose-6-phosphatase Activity of Intact Liver Microsomes, *The Journal of Biological Chemistry* Vol. 273, No. 11, 1998, pp. 6223-6227.
- [41]<http://www.originlab.com>, accessed in September 2007.
- [42]APHA. American Public Health Association. Standard Methods for the Examination of Water and Wastewater. 21st Ed., USA, Ed. American Public Health Association, 2005.
- [43]J. M. Cleaves, S L. Miller, Oceanic protection of prebiotic organic compounds from UV radiation, *Proceedings of the National Academy of Sciences of the United States of America*, Vol. 95, 1998, pp. 7260-7263.
- [44]J. B. Souza, L. A. Daniel, Comparison between sodium hipoclorite and peracetic acid for *E. coli*, coliphagis and *C. perfringens* inactivation of high organic matter concentration water, *Engenharia Sanitária e Ambiental*, Vol. 10, No. 2, 2005, pp. 111-117.
- [45]P.W. Atkins, *Physical Chemistry*, Oxford, 3rd edn, 1988.
- [46]R.J. Silbey, R.A. Alberty, *Physical Chemistry*, New York, Third Edition, 2001.
- [47]E. Puzenat, H. Lachheb, M. Karkmaz, A. Houas, C. Guillard, J.M. Herrmann, Fate of nitrogen atoms in the photocatalytic degradation of industrial (congo red) and alimentary (amaranth) azo dyes. Evidence for mineralization into gaseous dinitrogen, *International Journal of Photoenergy*, Vol. 5, 2003, pp. 51-58.
- [48]N. Genç, Photocatalytic oxidation of a reactive azo dye and evaluation of the biodegradability of photocatalytically treated and untreated dye, *Water SA*, Vol. 30, No. 3, 2004, pp. 399-405.
- [49]S. GUL, O. Serinda, H. Boztepe, Effects of Ozonation on COD Elimination of Substituted Aromatic Compounds in Aqueous Solution, *Turkish Journal of Chemistry*, Vol. 23, 1999, pp. 21-26.
- [50]M.M. Tauber, G.M. Guebitz, A. Rehorek, Degradation of azo dyes by laccase and ultrasound treatment, *Applied Environmental Microbiology*, Vol. 71, No. 5, 2005, pp. 2600-2607.
- [51]J.-W. Wegener, H. Schulz, Characterization of leather candidate certified reference materials for their mass fractions of aromatic amines, *Accreditation and Quality Assurance*, Vol. 12, 2007, pp. 12-20.
- [52]P.P. Vijaya, S. Sandhya, Decolorization and Complete Degradation of Methyl Red by a Mixed Culture, *The Environmentalist*, Vol. 23, 2003, pp. 145-149.
- [53]S.-A. Ong, E. Toorisaka, M. Hirata, T. Hano, Treatment of methylene blue-containing wastewater using microorganisms supported on granular activated carbon under packed column operation *Environmental Chemistry Letters*, Vol. 5, 2007, pp. 95-99.
- [54]J. Kirschbaum, C. Krause, H. Brückner, Liquid chromatographic quantification of synthetic colorants in fish roe and caviar, *European Food Research Technology*, Vol. 22, 2005, pp. 572-579.